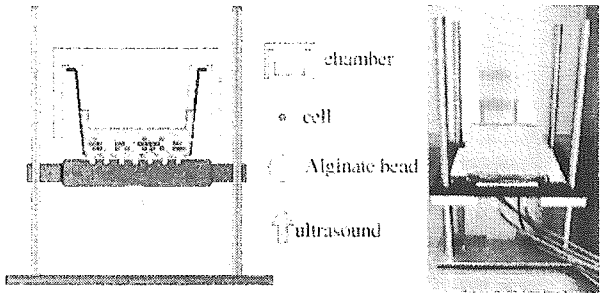

Fig. 2. Illustration of ultrasonic stimulation of cells. Ultrasound was transmitted through the bottom of the wells via coupling gel between the ultrasonic transducer and the plate. The diameter of ultrasound transducers was the same as that of the wells.

2.4. Evaluation

2.4.1. Measurement of DNA synthesis

The DNA synthesis was examined by the uptake of [^{3}H]-thymidine. At days 5 and 12 after the daily US stimulation, the media of each plate was changed, to complete medium containing [^{3}H]-thymidine at concentration of 2 μCi/ml. After 18 h from the start of labeling, beads were washed twice with PBS and were added to sodium citrate solution (55 mM, in 90 mM NaCl). The beads were dissolved and the two compartments (cell associated matrix (CM) and further removed matrix (FRM)) separated on mild centrifugation at 100*g* for 10 min at 4 °C. Then 10% trichloroacetic acid (TCA) was added to each fraction. The fractions were centrifuged (3000 rpm for 10 min) and the supernatant (TCA) was removed. This procedure was repeated five times, and TCA-insolvable material was collected and dried with 70% ethanol. The dry material was treated overnight with 1 ml of solvent (Solvable^{TM}; Packard, Meriden, CT) at 45 °C and 10 ml of liquid scintillation cocktail (AtomlightTM; Packard) was added for counting of emissions (Beckman LS4800, Fullerton, CA) [13,14]. Radioactivity (in disintegrations per minute [DPM]) of these results was divided by the amount of DNA calculated using Hoechst 33258 dye method. All the isotope experiments were repeated more than two times.

2.4.2. Measurement of PG synthesis

The incorporation of [^{35}S]-sulfate was used to measure PG synthesis. At the indicated times, cultures were labeled, to complete medium containing [^{35}S]-sulfate at concentration of 40 μCi/ml for 18 h. Subsequent PBS washes, dissolving alginate, TCA treatment, drying, scintillation counting were carried out with the same procedure as for [^{3}H]-thymidine uptake.

2.4.3. Measurement of DNA content

DNA content was measured using the fluorometric method as described previously. On day 0, 5, and 12 after US stimulation, beads of each well were collected and were dissolved by sodium citrate solution (55 mM, in 90 mM NaCl) for 10 min at 4 °C. After centrifugation, separated CM fractions were digested for 18 h at 55 °C in papain solution (20 μg/ml in 50 mM EDTA, 5mM L-cystein). 100 μl of Hoechst 33258 dye solution (1 μg/ml, pentahydrate, USA, Molecular Probes) was mixed with the digested sample and 2 h later, the emission spectrum of the mixture was determined for an excitation at 365 nm by measuring fluorescence emission of 460 nm using plate reader (FL500, Bio-Tek). The standard curve was determined using a known concentration of calf thymus DNA (Sigma) [15].

2.4.4. Measurement of PG content

PG content was accumulated by dimethylmethylene blue (DMMB, Polysciences, Inc.) assay [16]. Starting US at day 5 and 12, the beads were harvested, dissolved, and the two matrix compartments, CM and FRM, separated as described above. Each fraction was digested with papain (concentration of papain: CM; 20 μg/ml, FRM; 40 μg/ml) at 55° C for 18 h. The digested sample solution (75 μl) was mixed with 25 μl of 2.88 M GuHCl solution and 200 μl of DMMB reagent in a 96-well plate, and immediately the absorbance at 530 nm and 595 nm was measured by a plate reader (SPECTRA MAX250, Molecular Devices). Purified bovine nasal septum-D1 PG (Sigma, USA) was used as a standard and the ratio of 530 nm/595 nm were calculated. Total amount of PG per well was normalized vs. the total amount of DNA per well.

2.4.5. Statistical analysis

All experiments were performed in triplicate. Results were expressed as mean ± standard deviation of three experiments. Statistical differences were assessed using two-way analysis of variance (ANOVA) with Fisher's PLSD test as a post hoc test. The statistical significance was set at $p<0.05$.

3. Results

3.1. [^{3}H]-thymidine incorporation

[^{3}H] uptake by both NP and AF cells was significantly upregulated on day 14 compared with day 7 (Fig. 3). For NP cells, there were significant increases in the 7.5 mW groups on day 5 after the start of US stimulation compared with the control group. On day 12 after the start of US stimulation, there was also a significant increase in the 7.5 mW groups compared with the control (7 days: 7.5 mW; 22.37×10^3 dpm/μg DNA, $p = 0.014$, 14 days: 7.5 mW; 40.14×10^3 dpm/μg DNA, $p = 0.0443$). For AF cells, there were significant increases in the 7.5, 15, and 30 mW groups on day 5 after the start of US stimulation compared with the control group (7 days: 7.5 mW; 19.00×10^3 dpm/μg DNA, $p = 0.053$, 15 mW; 17.87×10^3 dpm/μg DNA, $p = 0.0325$, 30 mW; 18.27×10^3 dpm/μg DNA, $p = 0.0176$). On day 12 after the start of US stimulation, there was also a significant increase in the 7.5 and 15 mW groups compared with the control (14 days: 7.5 mW; 31.68×10^3 dpm/μg DNA, $p = 0.0098$). Upregulation of DNA synthesis at low US intensities was confirmed by comparison of the effects at 7.5–30 mW on both NP and AF cells.

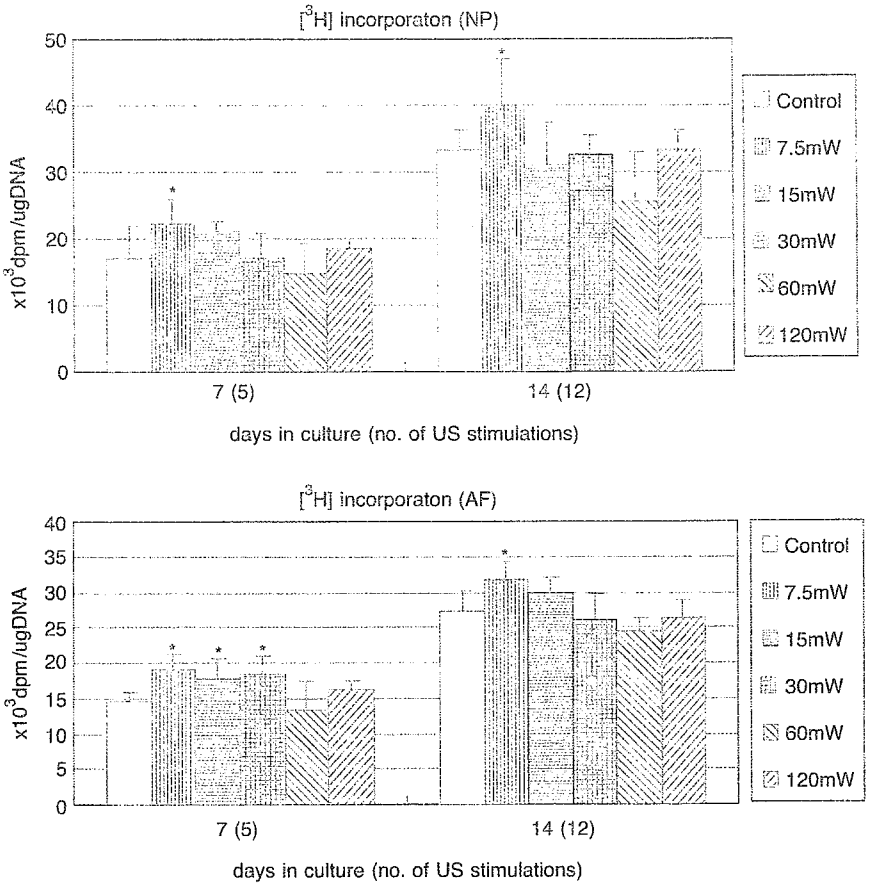

Fig. 3. Cell proliferation rate is expressed as [^{3}H]-thymidine incorporation divided by the DNA per well. For NP cells, there were significant increases in the 7.5 mW groups on day 5 after the start of ultrasound stimulation compared with the control group. For AF cells, there were significant increases in the 7.5, 15, and 30 mW groups on day 5 after the start of ultrasound stimulation compared with the control group. $p<0.05$.

3.2. *Hoechst 33258 assay*

There was a gradual increase of the DNA content through the 14-day culture period for both NP and AF cells (Fig. 4). In the case of NP cells, the DNA content was significantly increased in all US groups compared with the control group on day 5 after the start of US stimulation (7.5 mW; 4.86 μg/well, $p<0.001$, 15 mW; 4.84 μg/well, $p=0.041$, 30 mW; 4.15 μg/well $p=0.014$, 60 mW; 4.29 μg/well, $p=0.006$, 120 mW; 4.10 μg/well, $p=0.019$). On day 12 after the start of US stimulation, there was also a significant increase in both the 7.5 and 15 mW groups compared with the control group (7.5 mW; 8.96 μg/well, $p=0.0009$, 15 mW; 9.22 μg/well, $p=0.002$). In the case of AF cells, there was a significant increase in the 7.5 and 15 mW groups compared with the control group on day 5 after the start of US stimulation (7.5 mW; 4.66 μg/well, $p<0.001$, 15 mW; 4.78 μg/well, $p<0.001$). Similarly, on day 12 after the start of US stimulation, there was also a significant increase in the 7.5 and 15 mW groups compared with the control group (7.5 mW; 10.18 μg/well, $p<0.001$, 15 mW; 9.68 μg/well, $p<0.001$). As for [^{3}H]-thymidine incorporation, upregulation of DNA synthesis at low US intensities was confirmed by comparison of the effects of intensities at 7.5 and 15 mW on both NP and AF cells.

3.3. *[^{35}S]-sulfate incorporation*

[^{35}S]-sulfate uptake was significantly upregulated on day 7 compared with day 14 in both NP and AF cells (Fig. 5). With regard to NP cells, there was a significant increase of [^{35}S]-sulfate incorporation in the 30 and 120 mW groups compared with the control group (7 days: 30 mW; 53.81×10^3 dpm/μg DNA, $p=0.035$, 120 mW; 57.29×10^3 dpm/μg DNA, $p=0.005$). On day 12, there was also a significant increase in the high-intensity 30, 60, and 120 mW groups compared with the control group (7 days: 30 mW; 78.64×10^3 dpm/μg DNA, $p<0.001$, 60 mW; 74.65×10^3 dpm/μg DNA, $p<0.001$, 120 mW; 78.83×10^3 dpm/μg DNA, $p<0.001$). With regard to AF

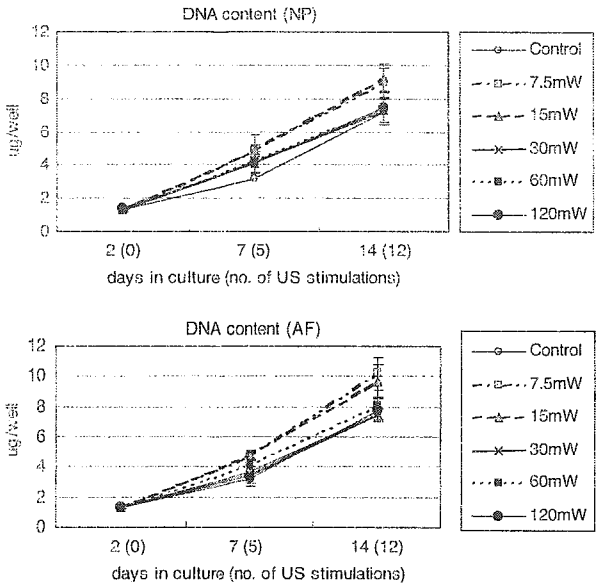

Fig. 4. Cell number is represented as the DNA content per well. In both NP and AF cells, the DNA content increased moderately until day 14. As for [^{3}H]-thymidine incorporation, upregulation of DNA synthesis at low ultrasound intensities was confirmed by comparison of the effects of intensities at 7.5 and 15 mW on both NP and AF cells. $p<0.05$.

cells on day 5 after the start of US stimulation, there was a significant increase of [^{35}S]-sulfate incorporation in the high-intensity 30, 60, and 120 mW groups compared with the control group (7 days: 30 mW; 80.35×10^3 dpm/μg DNA, $p<0.001$, 60 mW; 63.24×10^3 dpm/μg DNA, $p=0.0145$, 120 mW; 90.92×10^3 dpm/μg DNA, $p<0.001$). On day 12 after the start of US stimulation, there was also a significant increase in the 30, 60, and 120 mW groups compared with the control group (7 days: 30 mW; 115.8×10^3 dpm/μg DNA, $p<0.001$, 60 mW; 104.2×10^3 dpm/μg DNA, $p<0.001$, 120 mW; 113.9×10^3 dpm/μg DNA, $p<0.001$). At high intensities ranging from 30–120 mW, US stimulation upregulated PG synthesis by both NP and AF cells.

3.4. DMMB assay

The PG content was measured by the DMMB assay during culture of both NP and AF cells (Fig. 6). For NP cells, there was no significant difference between the control group and the US groups on day 5 after the start of US stimulation. On day 12 after the start of US stimulation, however, there was a significant increase of PG in the intensity 30 and 120 mW group compared with the control (control; 14.73 μg/μg DNA, 30 mW;

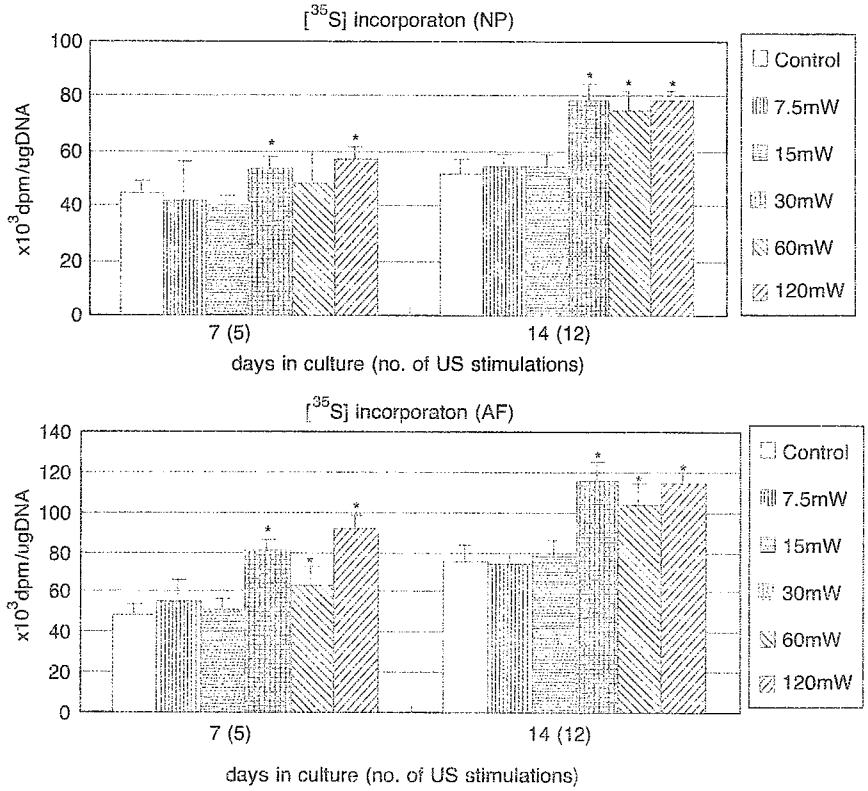

Fig. 5. PG synthesis per DNA in control and LIPUS groups' cultures. PG synthesis is expressed as [^{35}S]-sulfate incorporation per culture over a period of 18 h, divided by DNA content. At high intensities ranging from 30 to 120 mW, LIPUS stimulation upregulated PG synthesis in both NP and AF cells. $p<0.05$.

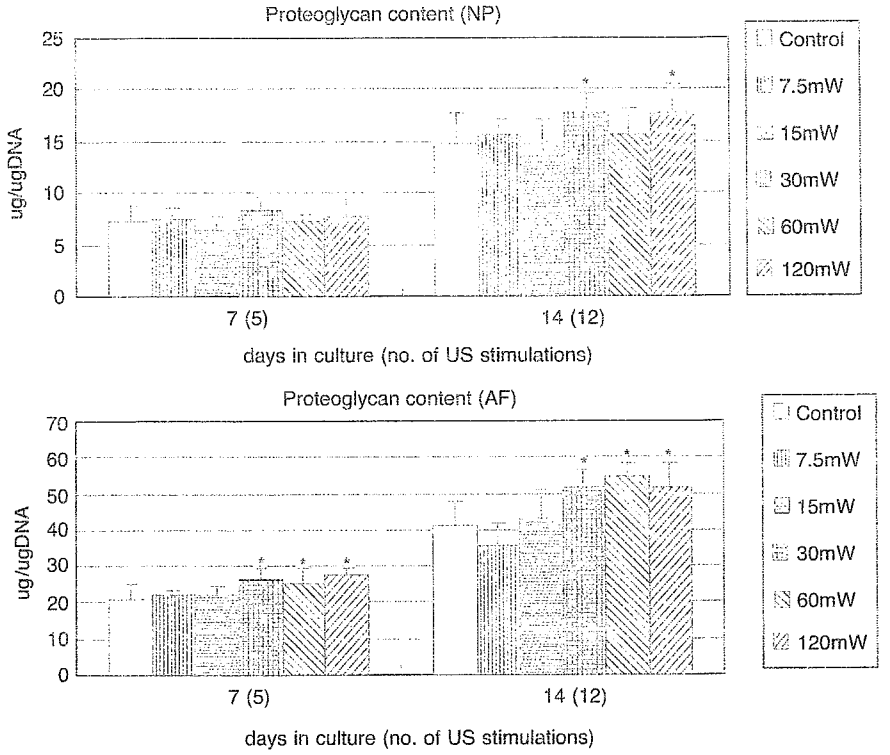

Fig. 6. At 7 and 14 days in culture, PG content of alginate beads was measured by DMMB assay. On day 5 after the start of LIPUS stimulation, for NP cells, there was no significant difference between the control group and the US groups. On day 12 after the start of ultrasound stimulation, there was a significant increase of PG content in high-intensity US groups, compared with the control. As with [^{35}S]-sulfate incorporation, in both NP and AF cells, there was also a significant increase in the high-intensity groups (30–120 mW) compared with the control group. $p<0.05$.

17.72 μg/μg DNA, $p = 0.0398$, 120 mW; 17.73 μg/μg DNA, $p = 0.0386$). For AF cells, there was a significant increase of PG in the high-intensity 30, 60, and 120 mW groups compared with the control group on day 5 after the start of US stimulation (30 mW; 26.35 μg/μg DNA, $p = 0.0044$, 60 mW; 25.29 μg/μg DNA, $p = 0.0184$, 120 mW; 27.40 μg/μg DNA, $p = 0.001$). On day 12 after the start of US stimulation, there was also a significant increase of PG in the high-intensity 30, 60, and 120 mW groups compared with the control group (30 mW; 51.47 μg/μg DNA, $p = 0.0075$, 60 mW; 54.35 μg/μg DNA, $p = 0.001$, 120 mW; 51.46 μg/μg DNA $p = 0.0075$). As with [^{35}S]-sulfate incorporation, there was also a significant increase in the high-intensity groups (30–120 mW) compared with the control group shown by the DMMB assay.

4. Discussion

In 1999, Javad et al. stimulated rat chondrocytes with LIPUS for 5 days, and reported that PG synthesis was promoted by an increase of aggrecan mRNA [11]. In 2002, it was reported that calcium ion signaling was necessary for LIPUS to stimulate aggrecan synthesis [17]. Another study showed that stimulation of chondrocytes by LIPUS caused an increase of type II collagen mRNA, while type X collagen mRNA was decreased, indicating a positive effect of LIPUS on chondrocytes [18].

From these reports, it was presumed that LIPUS has a similar effect on IVD cells to its action on cartilage cells, since disc cells are said to have a phenotype closer to that of cartilage cells. In addition, the decrease of the disc water content in the early stage of IVD degeneration, which is one of the factors causing low-back pain, depends on the content of PG. Therefore, it was demonstrated that upregulation of PG synthesis is fully applicable as a treatment for IVD degeneration.

With regard to [^{3}H]-thymidine incorporation, there was no overall difference between the control group and the US groups, but there was a significant increase in the low-intensity US groups (7.5 and 15 mW/cm^2) after 7 days of stimulation. In a series of experiments by Zhang et al. [18], chondrocytes were stimulated with US and there was an increase of cell proliferation after 3 days of low-intensity US. These findings are similar to results of the present study, suggesting that low-intensity US promotes cell proliferation even in the IVD. There have been many studies in which monolayer cultured cells were stimulated by LIPUS and chondrocytes or IVD cells are known to readily dedifferentiate in monolayer

cultures. In contrast, Chiba et al. [19] performed three-dimensional culture of alginate cells and maintained the morphology of the IVD cells during culture. The same procedure was also used in this study, with the objective being to create an environment as close as possible to the in vivo setting.

The [^{35}S]-sulfate incorporation data showed that US stimulation upregulated PG synthesis by NP and AF cells. With regard to the intensity of US, there was a significant increase compared with the control group at intensities of 30, 60, and 120 m W/cm^2. In addition, it was confirmed by the DMMB assay that the PG content of the US groups was significantly increased compared with the control group. However, NP cells showed no significant difference between the US groups and the control group at 7 days after the start of stimulation. This may have been due to the fact that NP cells are heterogeneous and have very low metabolic activity [2]. The NP that was used was immature, and therefore notochordal cells remained. The phenotype of the notochordal cells may have affected the results.

Low-intensity US is effective in promoting bone union [10], and is presently being used clinically for non-union of fractures. There is still an uncertainty about its mechanism of action, but stimulation of tissues by minute vibrations, improved capillary circulation, and increased permeability of the cell membrane have been reported [20]. The IVD is mechanically stimulated by constant pressure and stretching, so it may not be surprising for some positive effect to arise in the disc cells when the extracellular substrate is subjected to US vibration. In support of this, there are many reports about upregulation of PG synthesis when IVD cells are subjected to mechanical pressure such as hydrostatic pressure [21,22]. Conversely, there are reports that PG synthesis is downregulated when cells are cultured under zero gravity [23]. Accordingly, it seems that mechanical stimulation is likely to trigger an increase in the activity of IVD cells and that LIPUS is another trigger.

It is a significant point that cells used in this study were normal cells rather than cells from degenerating IVDs. Because the activity of cells from degenerating discs is low, it is unclear whether the same results would have been obtained with such cells. In addition, the cells forming the NP differ according to age, species, and extent of IVD degeneration, so the results obtained under other conditions will not necessarily be completely the same as those of this study. However, there have been no previous reports about US stimulation of IVD cells, so this investigation was designed as a preliminary study, and the IVDs of immature rabbits, which have been used in many experiments on the IVD that have already been published, were selected for analysis. There was no clear answer obtained about the level of US that produces the maximum efficacy. Although PG synthesis was increased by the comparatively high intensities of 30, 60, and 120 m W/cm^2, the exposure time was fixed at 20 min, so there remains the possibility that the same results could be obtained by longer stimulation at a lower intensity. Cell proliferation is increased at a comparatively low intensity. However, treating IVD degeneration requires therapy for the decreased water content of the disc in the early stage of degeneration and the decreased cell count throughout the disc, rather than a simple increment of cell proliferation. Therefore, intensifying the upregulation of PG synthesis may lead to a higher therapeutic efficacy.

The effect of LIPUS shown by this study was inferior to that seen in other studies on stimulation of the IVD using methods such as growth factors or coculture [14,24,25]. LIPUS also increases the sensitivity of cells to cytokines, so a synergistic effect may be expected. In addition, US is a safe and non-invasive procedure, and if it can be used for IVDs, it may become a new treatment for slowing the progression of IVD degeneration. Taking such positive effects of LIPUS into consideration, further studies on its application for the treatment of IVD degeneration need to be performed.

5. Conclusion

Rabbit intervertebral disc cells were stimulated by low-intensity ultrasound in vitro, and it was confirmed that cell proliferation and PG production was upregulated. These findings suggest the possibility of ultrasound becoming a new therapy for intervertebral disc degeneration.

Acknowledgements

Authors thank the staff at the Center for Education and Research, Tokai University School of Medicine. This work was supported in part by Grant-in-Aid for scientific research grant numbers 16390443, 15591605 and a Grant of The Science Frontier Program from the Ministry of Education, Culture, Sports, Science, and Technology of Japan, and a grant from 2004 Tokai University School of Medicine Research Aid.

Reference

[1] Luoma K, Riihimaki H, Luukkonen R, Raininko R, Viikari-Juntura E, Lamminen A. Low back pain in relation to lumbar disc degeneration. Spine 2000;25:487–92.
[2] Gruber HE, Hanley Jr EN. Analysis of aging and degeneration of the human intervertebral disc. comparison of surgical specimens with normal controls. Spine 1998;23:751–7.
[3] Ariga K, Miyamoto S, Nakase T, Okuda S, Meng W, Yonenobu K, Yoshikawa H. The relationship between apoptosis of endplate chondrocytes and aging and degeneration of the intervertebral disc. Spine 2001;26:2414–20.

[4] Phillips FM, An H, Kang JD, Boden SD, Weinstein J. Biologic treatment for intervertebral disc degeneration. Spine 2003;28:599.
[5] Walsh AJ, Bradford DS, Lotz JC. In vivo growth factor treatment of degenerated intervertebral discs. Spine 2004;29:156–63.
[6] Nishida K, Kang JD, Suh JK, Robbins PD, Evans CH, Gilbertson LG. Adenovirus-mediated gene transfer to nucleus pulposus cells. implications for the treatment of intervertebral disc degeneration. Spine 1998;23:2437–42.
[7] Kawakami M, Matsumoto T, Hashizume H, Yoshida M, Kuribayashi K. Osteogenic protein (OP-1/BMP7) inhibits degeneration and pain-related behavior induced by chronically compressed nucleus pulposus in the rabbit. Orthop Res Soc Trans 2004;29:80.
[8] Nomura T, Mochida J, Okuma M, Nishimura K, Sakabe K. Nucleus pulposus allograft retards intervertebral disc degeneration—an in vivo experimental study. Clin Orthop 2001;389:94–101.
[9] Sakai D, Mochida J, Yamamoto Y, Nomura T, Okuma M, Nishimura K, Nakai T, Ando K, Hotta T. Transplantation of mesenchymal stem cells embedded in Atelocollagen gel to the intervertebral disc: a potential therapeutic model for disc degeneration. Biomaterials 2003;24:3531–41.
[10] Duarte LR. The stimulation of bone growth by ultrasound. Arch Orthop Trauma Surg 1983;101:153–9.
[11] Parvizi J, Wu CC, Lewallen DG, Greenleaf JF, Bolander ME. Low-intensity ultrasound stimulates proteoglycan synthesis in rat chondrocytes by increasing aggrecan gene expression. J Orthop Res 1999;17:488–94.
[12] Zhang ZJ, Huckle J, Francomano CA. Spencer RGThe influence of pulsed low-intensity ultrasound on matrix production of chondrocytes at different stages of differentiation: an explant study. Ultrasound Med Biol 2002;28:1547–53.
[13] Uchiyama Y, Tamaki T, Fukuda H. Relationship between functional deficit and severity of experimental fast-strain injury of rat skeletal muscle. Eur J Appl Physiol 2001;85:1–9.
[14] Yamamoto Y, Mochida J, Sakai D, Nakai T, Nishimura K, Kawada H, Hotta T. Upreguration of the viability of nucleus pulposus by bone marrow-derived stromal cells. Spine 2004;29:1508–14.
[15] Kim YJ, Sah RL, Doog JY, Grodzinsky AJ. Fluorometric assay of DNA in cartilage explants using Hoechst 33258. Anal Biochem 1988;174:168–76.
[16] Brian OE, Dan LB, David AL. Quantification of sulfated glycosaminoglycans in chondrocyte/alginate culture, by use of 1,9-dimethylmethylene blue. Anal Biochem 1996;243:189–91.
[17] Parvizi J, Parpura V, Greenleaf JF, Bolander ME. Calcium signaling is required for ultrasound stimulated aggrecan synthesis by rat chondrocytes. J Orthop Res 2002;20:51–7.
[18] Zhang ZJ, Huckle J, Francomano CA, Spencer RG. The effects of pulsed low intensity ultrasound on chondrocyte viability, proliferation, gene expression and matrix production. Ultrasound Med Biol 2003;29:1645–51.
[19] Chiba K, Andersson GB, Masuda K, Thonar EJ. Metabolism of the extracellular matrix formed by intervertebral disc cells cultured in Alginate. Spine 1997;22:2885–93.
[20] Lehmann JF. Biophysical basis of biologic ultrasonic reactions with special reference to ultrasonic therapy. Arch Phys Med Rehabil 1953;34:139–52.
[21] Hutton WC, Elmer WA, Boden SD, Hyon S, Toribatake Y, Tomita K, Hair GA. The effect of hydrostatic pressure on intervertebral disc metabolism. Spine 1999;24:1507–15.
[22] Kasra M, Goel V, Martin J, Wang ST, Choi W, Buckwalter J. Effect of dynamic hydrostatic pressure on rabbit intervertebral disc cells. J Orthop Res 2003;21:597–603.
[23] Okuma M, An H, Thonar E, Sah RL, Pichica R, Yamada M, Imai Y, Masuda K. Microgravity stimulates cell proliferation but suppresses proteoglycan metabolism. Ortho Res Soc Trans 2003, poster #0355.
[24] Tim Yoon S, Su Kim K, Li J, Soo Park J, Akamaru T, Elmer WA, Hutton WC. The effect of bone morphogenetic protein-2 on rat intervertebral disc cells in vitro. Spine 2003;28:1773–80.
[25] Masuda K, Takegami K, An H, Kumano F, Chiba K, Andersson GB, Schmid T, Thonar E. Recombinant osteogenic protein-1 upregulates extracellular matrix metabolism by rabbit annulus fibrosus and nucleus pulposus cells cultured in alginate beads. J Orthop Res 2003;21:922–30.

Available online at www.sciencedirect.com
SCIENCE DIRECT®
Biomaterials 27 (2006) 346–353
Biomaterials
www.elsevier.com/locate/biomaterials

Atelocollagen for culture of human nucleus pulposus cells forming nucleus pulposus-like tissue in vitro: Influence on the proliferation and proteoglycan production of HNPSV-1 cells

Daisuke Sakai[a,b,*], Joji Mochida[a,b], Toru Iwashina[a,b], Takuya Watanabe[a,b], Kaori Suyama[a,b], Kiyoshi Ando[b], Tomomitsu Hotta[b]

[a]*Department of Orthopaedic Surgery, Surgical Science, Tokai University School of Medicine, Bohseidai, Isehara, Kanagawa 259-1193, Japan*
[b]*Research Center for Regenerative Medicine, Tokai University School of Medicine, Bohseidai, Isehara, Kanagawa 259-1193, Japan*

Received 28 June 2005; accepted 30 June 2005
Available online 18 August 2005

Abstract

Nucleus pulposus (NP) is responsible for maintaining function and structure of the disc. Scaffolds to culture disc cells three-dimensionally are emphasized in recent reports on development of a new method for treating disc degeneration using cell transplantation and tissue engineering. Among artificial scaffolds and cell carrying materials, Atelocollagen is a collagen gel that has an advantage in safety issues over others. However, to date there has been no study that investigated culture of human nucleus pulposus cells in Atelocollagen. To investigate whether Atelocollagen could be used as a culture scaffold and if it has any effect on cell proliferation and proteoglycan (PG) production, as well as to find the optimal commercially available Atelocollagen for NP cell transplantation and tissue engineering, we cultured human NP cell line HNPSV-1, in three different Atelocollagen and compared with alginate. Furthermore, NP-like tissues were generated using these cells and different Atellocollagen solutions. Results showed that both DNA synthesis and content is significantly greater when cultured in Atelocollagen than in alginate. On the other hand, proteoglycan synthesis and accumulation was significantly greater in alginate compared with the 0.3% Atelocollagen scaffolds; with 3% Atelocollagen, however, results were similar. NP-like tissue generated by Atelocollagen showed good water and proteoglycan preservation. The current study demonstrates that the use of Atelocollagen as an in vitro culture scaffold for three-dimensional culture of human NP cell lines is indeed feasible and moreover, Atelocollagen possesses the potential to become a candidate scaffold for cell transplantation or tissue engineering for the treatment of intervertebral disc degeneration.
© 2005 Elsevier Ltd. All rights reserved.

Keywords: Intervertebral disc; Disc degeneration; Nucleus pulposus; Atelocollagen; Tissue engineering; Scaffold

1. Introduction

The nucleus pulpous (NP) plays an important role in preserving structure and function of the intervertebral disc (IVD) [1–3]. There are many reports in the literature that claim that the decrease in cell number in the nucleus due to multiple factors (malnutrition, mechanical stress and apoptosis, among others) leads to subsequent loss of proteoglycan (PG)-rich matrix, resulting in degeneration [4,5]. However, due to the lack of cellular resources, there have been few studies of the character and function of human NP cells [6,7]. Therefore, more studies of these cells from the human NP are needed.

NP cells are a heterogeneous population composed of at least two different cell types: notochordal cells and chondrocyte-like cells. The number of notochordal cells tends to decrease with age and in most human adults chondrocyte-like cells show dominance. Like

*Corresponding author. Department of Orthopaedic Surgery, Surgical Science, Tokai University School of Medicine, Bohseidai, Isehara, Kanagawa 259-1193, Japan. Tel.: +81 463 96 1121; fax: +81 463 96 4404.
E-mail address: daisakai@is.icc.u-tokai.ac.jp (D. Sakai).

0142-9612/$ - see front matter © 2005 Elsevier Ltd. All rights reserved.
doi:10.1016/j.biomaterials.2005.06.040

chondrocytes, the majority of human NP cells show spherically shaped morphology and a chondrocyte-like phenotype when cultured in three-dimensional culture systems [8]. Since it is understood that NP cells dedifferentiate under two-dimensional culture conditions, various materials have been suggested for culturing these cells in three-dimensional conditions [9–11].

Alginate, agarose, collagen gel, collagen sponges and fibrin gels were used in previous studies to hold cells in three-dimensional culture systems [11]. Besides their value as in vitro culture scaffolds, such scaffolds are further expected to be useful as candidates for cell carriers in cell transplantation therapy for IVD degeneration or cell scaffolds in IVD tissue engineering. Autologous or allogenic disc cell transplantation has been reported from multiple research groups as a major approach in delaying the progression of degeneration by restoring lost cells [12–16]. In delivering donor cells to the IVD, the selection of an adequate cell carrier is important. The generation of disc-like tissue using various scaffolds and tissue-engineering techniques also possesses the potential of becoming a new strategy for regenerating the disc [17–19].

Among artificial scaffolds and cell-carrying materials, Atelocollagen is a collagen gel that has an advantage in safety, as the antigenic telopeptide region has been removed by pepsin digestion and differential salt precipitation during purification. Atelocollagen is in liquid form at 4 °C, but gels after incubation at 37 °C. Atelocollagen composed of type I collagen purified from calf dermis is already in use by physicians for subcutaneous injection during cosmetic and plastic surgery [20]. Atelocollagen can be obtained as collagen types I–IV, depending on the animal and organ from which it is purified.

In this study, we cultured the human NP cell line HNPSV-1, established in our laboratory [21], in 0.3% and 3% type I Atelocollagen and 0.3% type II Atelocollagen. The aim was to investigate whether Atelocollagen could be used as a culture scaffold and if it has any effect on cell proliferation and proteoglycan (PG) production, as well as to find the optimal commercially available Atelocollagen for NP cell transplantation and tissue engineering. The results were compared with an alginate culture system. Furthermore, we generated NP-like tissue by 4-week culture of human NP cells in these three different Atelocollagens and evaluated water and PG accumulation, along with histology.

2. Materials and methods

All experimental protocols were approved by Institutional Review Board and Animal Experimentation Committee of the author's institution.

2.1. Cell culture in Atelocollagen gels and alginate

Cryopreserved human NP HNPSV-1 cells, established from a NP from a 19-year-old female, were used for the study. Types I and II Atelocollagen (0.3%, pH 3.0, Koken, Tokyo, Japan) were prepared for cell culture by adding 1 ml of 10 × concentrated Dulbecco's modified Eagle's medium (DMEM, Gibco-BRL, Grand Island, NY), 0.1 ml of 10 mM HEPES buffer, 0.1 ml of 10 mM $NaHCO_3$, and 0.8 ml of distilled water to 8 ml of 0.3% Atelocollagen solution to make 10 ml of a 0.24% solution (pH 7.4) as described by Uchio et al. [22]. In addition, 1 ml of 10 × concentrated DMEM, and 1 ml of 2.2% $NaHCO_3$ with 0.05 N NaOH and 200 mM HEPES were added to 8 ml of 3% type I Atelocollagen to make 2.4% Atelocollagen solution, following the method by Ochi et al. [23]. For alginate culture, 1.2% sodium alginate solution (Cambrex, East Rutherford, NJ) dissolved in 150 mmol/L NaCl was also prepared. No medium was added to alginate solution following the formulation of previous studies using alginate culture system [9].

HNPSV-1 cells were mixed in these four solutions at a final cell density of 10^6 cells/ml and cultured three-dimensionally in culture inserts (Becton Dickinson, BD, Franklin Lakes, NJ) and 12-well culture plates (BD) to make cell/Atelocollagen or cell/alginate constructs. Non-cell-seeded solution (200 μl) was added first to avoid cell attachment to the bottom of the insert, followed by overlaying with 500 μl of cell mixed solution. Gelation of Atelocollagen was performed by incubation at 37 °C in a 5% CO_2 atmosphere for 1 h, and alginate by temporal exposure to a 102 mM/L calcium chloride solution. After complete gelation, 300 μl of DMEM with 20% fetal bovine serum (FBS, Gibco), penicillin (100 μg/ml) and streptomycin (250 ng/ml), was added to the insert and 1 ml to the outer well. Cultures were maintained for up to 14 days, with medium changed every 48 h, and six inserts were evaluated on each of days 3, 7 and 14.

2.2. Cell morphology

The morphology of the HNPSV-1 cells was examined using light microscopy at each evaluation time point.

2.3. Evaluation of cell proliferation

Cellular proliferation was evaluated by measuring the uptake of [^{3}H]-thymidine into newly synthesized DNA after 72 h of culture and, further, by measuring the DNA content at each evaluation period.

2.3.1. DNA synthesis

After 48 h of culture, cells were fed for the last 24 h with DMEM containing [^{3}H]-thymidine (Amersham, Piscataway, NJ) at concentration of 2 μCi/ml per well for 24 h. Constructs with embedded cells were digested for 18 h at 55 °C in a papain solution (20 μg/ml in 50 mM EDTA, 5 mM L-cysteine). The digests were washed twice with phosphate buffered saline (PBS) and 2 ml of 10% trichloroacetic acid (TCA) was added to each well. In alginate culture, cells and matrix components were released from alginate using dissolving buffer (55 mmol/L Na-citrate and 150 mmol/L NaCl) followed by PBS wash and

addition of TCA. Cultures were centrifuged (3000 rpm for 10 min), and the supernatant removed. This procedure was repeated five times, and the TCA-insoluble material was collected and dried with 70% ethanol. The dried material was treated overnight with 1 ml of solvent (Solvable, Packard, Meriden, USA) at 45 °C and 10 ml of liquid scintillation cocktail (Atomlight, Packard, Meriden, USA) was added (Beckman LS4800, Fullerton, USA). The radioactivity of the samples, in disintegrations per minute (DPM), was divided by their DNA content, quantified as described below. The radioactivity of each sample was expressed as DPM per μg DNA.

2.3.2. DNA content

To measure the DNA content, constructs were enzymatically digested with 0.25% collagenase type II (Sigma) in DMEM for 1 hour at 37 °C to recover the HNPSV-1 cells from the Atelocollagen. Cells were released from alginate using dissolving buffer and recovered. Recovered cells were digested in a papain solution (20 μg/ml in 50 mM EDTA, 5 mM L-cysteine) for 18 h at 55 °C. The digests were mixed with 100 μl of bisbenzimidazole fluorescent dye (Hoechst 33258, Molecular Probes, Eugene, OR) and measured using a fluorometer, as previously described [24]. Calf thymus DNA (Sigma, St. Louis, MO) was used for the standard.

2.4. Evaluation of PG synthesis and accumulation

Evaluation of PG synthesis was performed by measuring newly synthesized PG by quantification of [^{35}S]-sulfate uptake after 72 h of culture, and the accumulation of PG determined by measuring the sulfated glycosaminoglycan (S-GAG) content at each time point.

2.4.1. PG synthesis

In order to measure the newly synthesized PG in Atelocollagen and alginate cultures, after 48 h of culture, cells were fed with DMEM containing [^{35}S]-sulfate (Amersham) at a concentration of 40 μCi/ml per well for 24 h. Atelocollagen cultures with medium and were digested for 18 h at 55 °C in a papain solution (20 μg/ml in 50 mM EDTA, 5 mM L-cysteine). Free non-incorporated [^{35}S]-sulfate was removed by $BaCl_2$ precipitation. Radioactivity of the supernatant was counted by scintillation counting. In alginate cultures, alginate cultures were washed with 0.9% NaCl containing 5 mmol/L of $CaCl_2$ and 5 mmol/L of Na_2SO_4 six times to remove free non-incorporated [^{35}S]-sulfate, and dissociated in ethylendiaminetetraacetic acid-sodium citrate before scintillation counting as previously described by others [8,25]. [^{35}S]-sulfate incorporation as described by DPM per μg DNA was obtained using the DNA measuring techniques written above.

2.4.2. PG accumulation

To assess PG accumulation, S-GAG content values in each of the constructs without medium were quantified by dimethylmethylene blue (DMMB, Sigma) dye assay. Briefly, constructs were digested using 10 times concentrated papain solution (200 μg/ml in 50 mM EDTA, 5 mM L-cysteine) for 24 h in 55 °C. Digested samples were mixed with DMMB buffer solution and measured spectrophotometrically, as previously described [26]. A standard curve was generated using purified nasal septum D1 PG (Sigma). An aliquot of papain digests were also used to measure DNA content, in order to obtain PG/ per μg DNA data.

2.5. Generation of NP-like tissue

For generation of NP-like tissue, 700 μl of HNPSV-1 cells embedded in three types of Atelocollagen (0.3% type I, II and 3% type I) at 10^6 cells/ml were individually set in sterile NP-shaped aluminum molds and placed in 10 cm plastic dishes. These cell-embedded constructs were cultured for 4 weeks with DMEM with 20% FBS, penicillin (100 μg/ml) and streptomycin (250 ng/ml) at 37 °C, in a 5% CO_2 atmosphere. Medium was changed every 72 h. Six specimens were generated for each Atelocollagen.

2.6. Measurement of wet and dry weight

Four of the NP-like tissues were weighed immediately after retrieval from culture, to give wet weight, and then lyophilized overnight and weighed to give dry weight. The water content of the tissues was determined by calculation of the percentage difference of the wet and dry weight values.

2.7. Tissue histology

Two specimens generated from each Atelocollagen were fixed in 10% formalin and paraffin embedded for histological sectioning. Sections were stained with hematoxylin and eosin, and toluidine blue.

2.8. PG accumulation in the tissue

The S-GAG content in four specimens generated from each Atelocollagen was evaluated using the methods described above. Data were expressed as μg S-GAG/mg dry weight.

2.9. Statistical analysis

Statistical analysis was performed by using Stat View software (ver. 5.0, Abacus Concepts, Berkeley, CA). The data were expressed as mean ± standard deviation. Comparison of group means was performed using Student's *t*-test with statistical significance determined based upon *P*-values of <0.05.

3. Results

3.1. Morphology of HNPSV-1 cells in Atelocollagen

Morphological analysis could not be performed for cells cultured in the 3% Atelocollagen due to its opacity after gelation. In the other cell-seeded constructs, the HNPSV-1 cells showed a spherical appearance, making small colonies, as are often seen in three-dimensional culture of human NP cells. However, there were

differences between constructs in the number of colonies and amount of extracellular matrix (ECM). Cells cultured in alginate showed abundant ECM-producing colonies. On the other hand, in the 0.3% type I and II Atelocollagens, most of the cells were spherical but with reduced colony formation (Fig. 1).

3.2. Cell proliferation

DNA synthesis as measured by uptake of [^{3}H]-thymidine measurement in the cell-seeded constructs showed significant uptake in 3% type I Atelocollagen and 0.3% type I Atelocollagen over alginate, with the lowest uptake. (3% type I Atelocollagen: 20414±3149, 0.3% type I Atelocollagen: 17980±5933, 0.3% type II Atelocollagen: 12357±1068 and alginate 10584±1172; all values expressed as DPM/μg DNA, Fig. 2a). DNA content measurement demonstrated similar results after 14 days of culture. A significant increase in DNA was achieved in Atelocollagen culture over the alginate (3% type I Atelocollagen: 48.53±4.8, 0.3% type I Atelocollagen: 35.4±3.5, 0.3% type II Atelocollagen: 28.8±2.6 and alginate 17.0±3.7; all values are expressed as μg/ml, Fig. 2b).

3.3. PG synthesis and accumulation

Results of PG synthesis, measured by uptake of [^{35}S]-sulfate, were significantly higher in the 1.2% alginate and 3% Atelocollagen than in the other matrices (alginate: 6448±8720, 3% type I Atelocollagen: 6003±5880, 0.3% type I Atelocollagen: 2349±3143, 0.3% type II Atelocollagen: 1510±589, Fig. 3a). PG accumulation, evaluated by measurement of S-GAG content, showed similar results, being significantly higher in the cells seeded in 1.2% alginate and 3% Atelocollagen after 14 days in culture (alginate: 116.7±6.8, 3% type I Atelocollagen: 68.8±3.1, 0.3% type I Atelocollagen: 37.1±3.9, 0.3% type II Atelocollagen: 32.7±2.5, all values expressed as μg/ml, $P<0.05$, Fig. 3b). Furthermore, when calculating S-GAG/DNA,

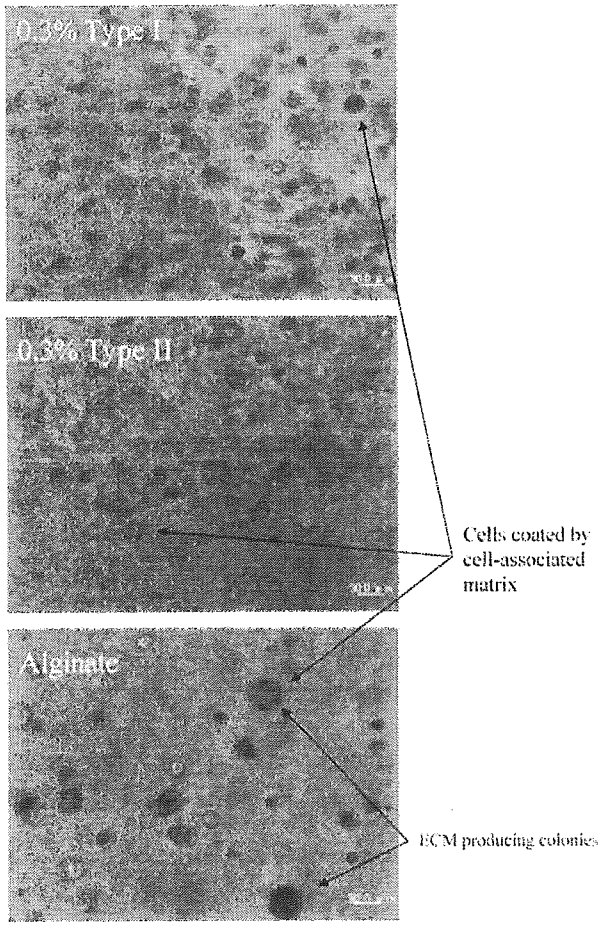

Fig. 1. HNPS-1 cells cultured for 5 days in Atelocollagen and alginate. HNPSV-1 cells express spherical appearance with colonization most frequently seen in alginate culture. Bar = 30 μm.

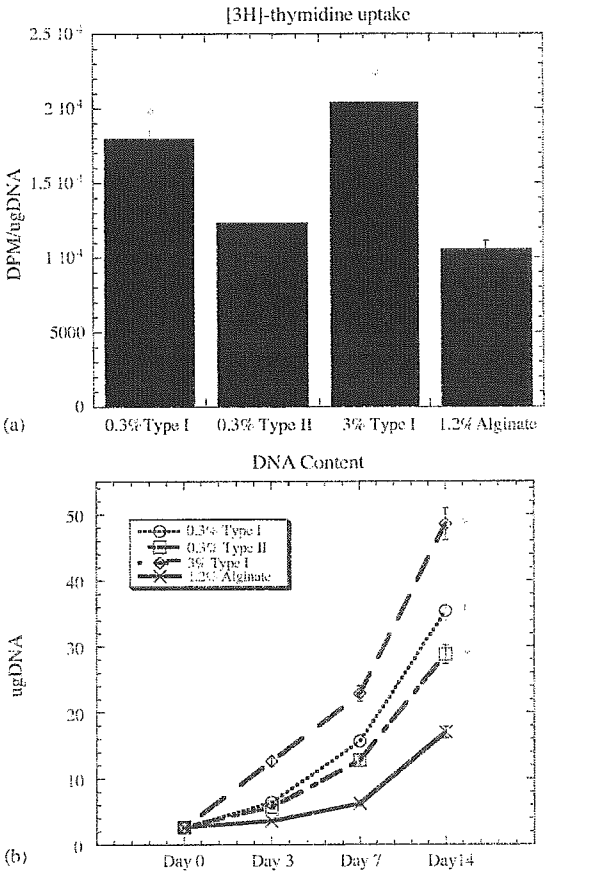

Fig. 2. Cell proliferation assays. (a) DNA synthesis after 3 days of culture showed significantly higher values in type I Atelocollagen gels. (b) DNA content resulted in significance in Atelocollagen cultures over alginate. $P<0.05$.

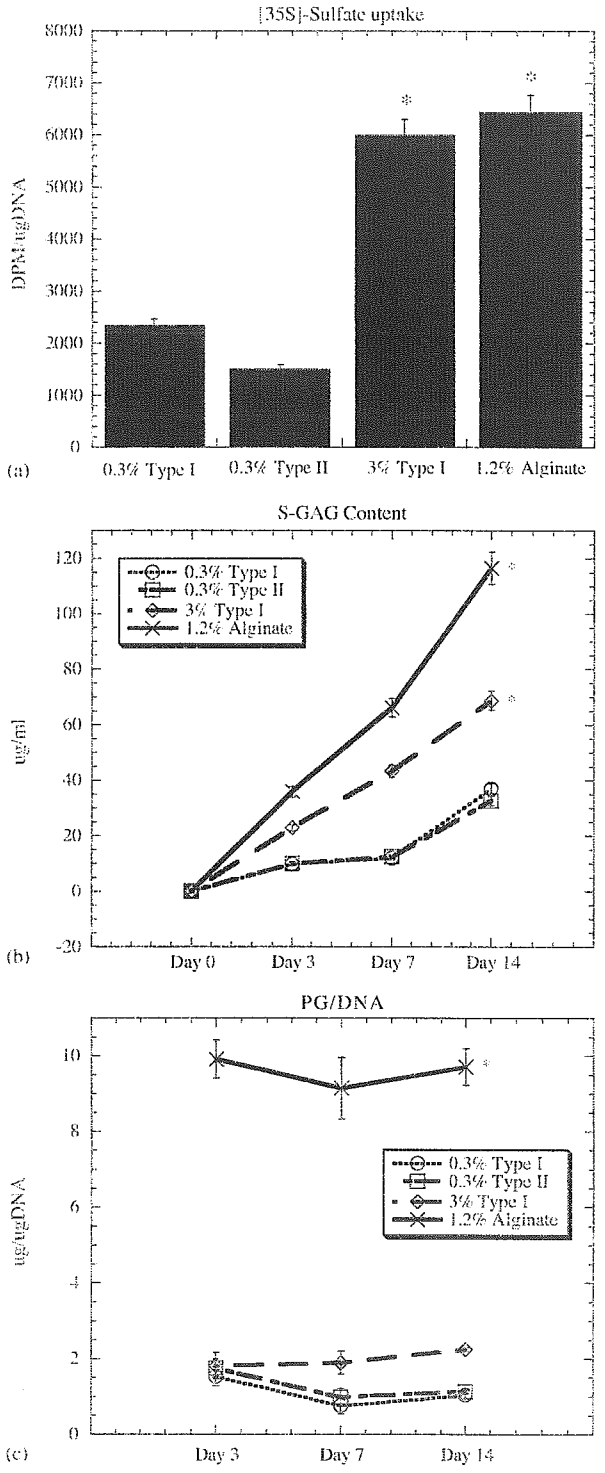

Fig. 3. PG production assays. (a) Alginate and 3% Atelocollagen cultures demonstrated significantly higher ability to synthesize PG over low concentrated Atelocollagen cultures. (b) S-GAG content also resulted in significance in alginate and 3% Atelocollagen cultures. However, in calculating PG content/DNA, alginate culture dominates others. $P<0.05$.

the results for the cells seeded in alginate were significantly higher than those in the Atelocollagen (Fig. 3c).

3.4. NP-like tissue formed in vitro by Atelocollagen

The gross findings for the NP-like specimens formed by the three types of Atelocollagen after 4 weeks of culture showed NP shaped tissue with differences in their gelatinous appearance, with tissues formed by type II Atelocollagen being most gelatinous (Fig. 4a). Tissue thickness was most prominent in the 3% type I Atelocollagen: 3.8 ± 1.5 mm compared to 3.3 ± 1.1 mm in the 0.3% type I Atelocollagen: and 2.2 ± 0.8 mm in the 0.3% type II Atelocollagen (Fig. 4b).

3.5. Tissue weight and water content of the generated tissue

The mean tissue dry weights were 2.2 ± 4.8 mg in the 0.3% type I Atelocollagen, 1.5 ± 3.5% in the 0.3% type II Atelocollagen, and 2.8 ± 8.9 in the 3% type I Atelocollagen specimens. Water contents, calculated from the dry and wet tissue weights, were 88 ± 3.5% in the 0.3% type I Atelocollagen, 92 ± 7.1% in the 0.3% type II Atelocollagen and 89 ± 6.8% in the 3% type I Atelocollagen (Fig. 5).

3.6. Histology

Histology of the tissues showed spherically shaped HNPSV-1 cells surrounded by rich layers of ECM. Toluidine blue staining of the tissue showed abundant positive staining in the ECM of all of the specimens,

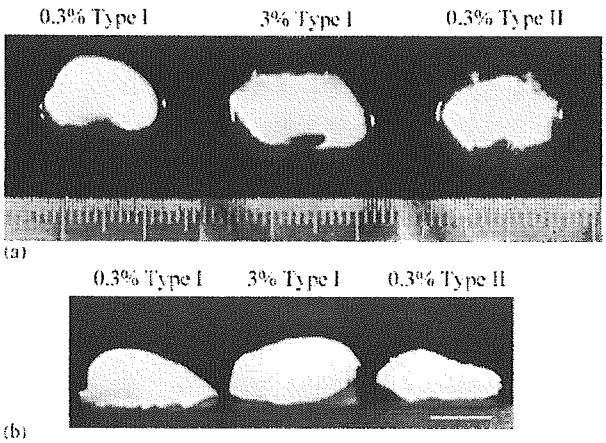

Fig. 4. NP-like tissues generated by HNPSV-1 cells embedded in Atelocollagen. (a) Gross finding of tissues showing 0.3% type II Atelocollagen being the most gelatinous. (b) However, in thickness, tissues made with type I Atelocollagens are more thick tan that by type II.

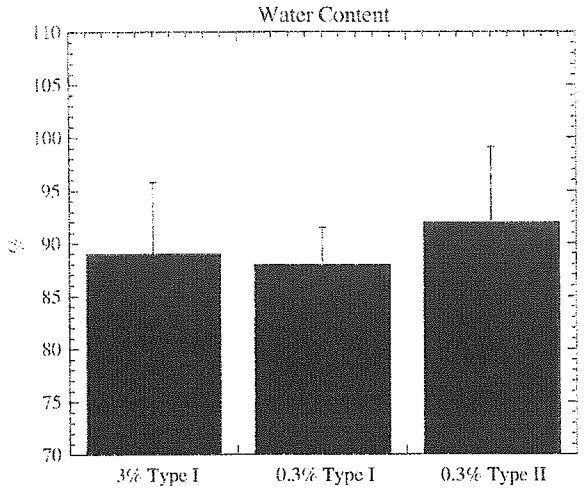

Fig. 5. Result of water content analysis of the generated NP-like tissues.

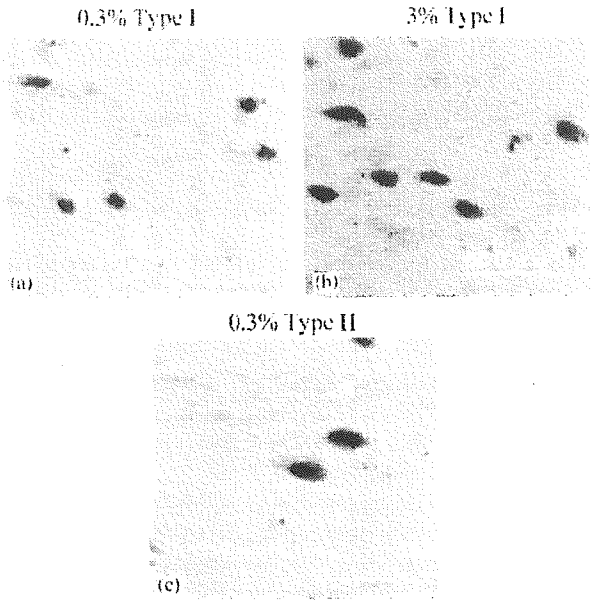

Fig. 6. Histological analysis by toluidine blue staining.

suggesting that sulfated PGS were being produced by HNPSV-1 cells after seeding (Fig. 6a–c).

3.7. PG accumulation

Measurement of the S-GAG content in these tissues showed that tissue formed in the 3% type I Atelocollagen contained significantly more S-GAG than the tissue formed in the other matrices (3% type I Atelocollagen, 336 ± 65.4; 0.3% type I Atelocollagen, 176 ± 52.3; 0.3% type II Atelocollagen, 120 ± 45.6; all values expressed as μg/mg dry weight; Fig. 7).

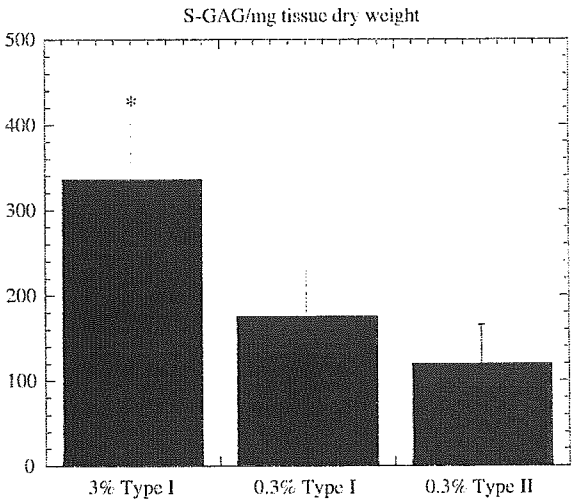

Fig. 7. Result of PG content per tissue dry weight of the generated NP-like tissues. $P < 0.05$.

4. Discussion

The results of the current study show that the use of Atelocollagen as an in vitro culture scaffold for three-dimensional culture of human NP cell lines is indeed feasible. However, compared with alginate culture, there were some differences in their influence on cell proliferation and PG production. Evaluation of cell proliferation showed that when cells are seeded in Atelocollagen scaffolds, both DNA synthesis and content is significantly greater than when cultured in alginate. On the other hand, PG synthesis and accumulation was significantly greater in alginate compared with the 0.3% Atelocollagen scaffolds. For 3% Atelocollagen, the results did not significantly change compared with alginate. From these results, one might suspect that, since alginate culture promotes more tight and intense holding of the cells, with reduced permeability compared to collagen lattices such as Atelocollagen, PG production ability is greatly dependent on actual holding and restricting of the cell. The fact that PG synthesis and production were significantly higher in the higher concentration of Atelocollagen provides strong evidence for this assertion, and measurement of PG secreted into the media might provide further clarification.

Differences in the type I and II Atelocollagens are also evident in the results of the current study. In comparison of the 0.3% type I and II Atelocollagens, type I presented higher values in all of the evaluations. However, in the gross findings and water content results, type II appeared most gelatinous and held the most water. From the fact that tissues generated by type II

Atelocollagen contained the least PG content, one might suspect that type II Atelocollagen itself holds more water than type I Atelocollagen. Type II Atelocollagen has a greater tendency to dissolve in aqueous conditions compared with type I Atelocollagen, due to the differences between type I and II collagen fibers. Type I Atelocollagen is purified from calf dermis and type II is from articular cartilage.

Formulation for adjustment of pH in Atelocollagen solutions before ongoing to cell seeding was obtained from previously described studies in the literature. Although large variation between 3% and 0.3% Atelocollagen solution was noted, there was no apparent influence of this difference in cell viability. However, there is a possibility that greater change in formulation may turn out to a different result.

Another point to consider is the great decrease in wet weight during the generation of NP-like tissue. Atelocollagen/cell construct just before setting into the mold weighs about 700 mg. However, at the time of recovery, these constructs weigh about 20–30 mg. This may be explained by the fact that Atelocollagen without cellular component dissolves in medium over time (about 2 weeks). Therefore, it is assumed that recovered tissues are mostly composed by seeded cells and secreted matrix.

In evaluation of tissue-engineered disc, it is most important to know whether the construct reached the S-GAG content level of the native nucleus. From results of the current study, in the NP-like tissue composed by 3% Atelocollagen, S-GAG content achieved about 30–35μg/mg wet weight. These data are remarkable since it shows that the construct achieved about 50–60% level of S-GAG content compared to the native NP in human adults [17,27]. It is apparent that generation of a NP-like tissue in vitro is a formidable challenge, and clearly needs more investigation. However, our result implies new hopes for applicability of the tissue-engineered disc for IVD repair. Perhaps culture condition that mimics in vivo environmental properties of native NP may be needed for cells to behave like the way they are in vivo.

Furthermore, we must be aware of limitations due to the use of a cell line in the current study. Culture studies using human NP cells have long been problematic due to a reduced opportunity to obtain tissue and the low cellularity and poor culture yields accounting for difficult in vitro expansion [28]. It is almost impossible to organize wide-scale in vitro studies using primary cultured human NP cells and, for that reason, there are only a few reports in the literature regarding human NP cells. The human NP cell line HNPSV-1 established from a young human's NP possesses the ability to express some of the major characteristics of human NP cells [21]. However, there certainly are limitations in using a cell line for studies aimed at native cells, since by establishing a prolonged cell life some major cell characteristics may be altered. For HNPSV-1 cells, it is known that cell proliferation is increased in monolayer culture and the karyotype of these cells shows some abnormalities. Nevertheless, cell proliferation and matrix production in three-dimensional conditions share similar patterns with native NP cells. Therefore, the results of the current study will be applicable to the application of Atelocollagen in culture of human NP cells.

Alterations of the structure and function of the IVD, the major cause of disc degeneration, is a great medical problem with no currently available methods for restoration. Spinal fusion surgeries have been shown to be effective in some cases [29]. However, eliminating mobility from the spine is unquestionably diverging from the biological nature of the human body. Artificial disc implantation has become another candidate for restoring disc function, but there are many limitations, as known from the use of artificial implants in other parts of the body [30]. Approaches to repair of the damaged disc biologically seem more appropriate. Cell transplantation therapy to decelerate the progression of disc degeneration has proven an effective strategy in animal models [12–16]. It is not known if a cell carrier is really needed for cell delivery, but owing to the IVD's contained structure, relatively non-solid constructs may well be applied in cell transplantation of the IVD. Recently, several groups have attempted to produce disc-like materials in vitro and in vivo for implantation [17–19]. Like many other tissue-engineering studies in various fields, selection of appropriate scaffold is a major factor in generating tissue-engineered discs. Moreover, safety issues exist, as most of the scaffolds have not been tested in humans. Sodium alginate is a common scaffold, often used to culture disc cells and chondrocytes in three-dimensional conditions. When compared with monolayer culture, ECM production is enhanced when these cells are cultured in alginate. Despite the fact that alginate culture shows significantly increased S-GAG content over Atelocollagen, biochemical analysis of native NP has shown that, in real situations, disc cells produce much more PG than cells cultured in alginate [31]. As a great advantage when considering clinical application, Atelocollagen has proven clinically to be a relatively safe material for implantation into the human body.

Although we cannot indicate the appropriate commercially available Atelocollagen for use in cell transplantation and tissue engineering, we can suggest that to obtain high PG synthesis and accumulation or for tissue engineering, where scaffolds must securely hold cells, highly concentrated solutions like 3% type I Atelocollagen are best suited. However, in order to achieve the largest water content and for delivery of cells to the contained disc space, 0.3% type II Atelocollagen might be beneficial.

In summary, the results of our study suggest that culture of human NP cells in Atelocollagen can provide three-dimensional culture condition for human NP cells, as measured by cell proliferation and PG production. Furthermore, Atelocollagen possesses the potential to become a candidate scaffold for cell transplantation or tissue engineering for the treatment of IVD degeneration.

Acknowledgements

Authors thank Akihiko Serizawa and Center for Education and Research, Tokai University School of Medicine for expert technical assistance. This work was supported in part by Grant-in-Aid for scientific Research grant numbers 16390443, 15591605 and a Grant of The Science Frontier Program from the Ministry of Education, Culture, Sports, Science and Technology of Japan, and a grant from 2004 Tokai University School of Medicine Research Aid.

References

[1] Nishimura K, Mochida J. Percutaneous reinsertion of the nucleus pulposus: an experimental study. Spine 1998;23:1531–638.
[2] Nishida K, Kang JD, Gilbertson LG, Moon S- H, Suh J- K, Vogt MT, Robbins PD, Evans CH. 1999 Volvo Award in basic science: modulation of the biologic activity of the rabbit intervertebral disc by gene therapy: an in vivo study of adenovirus-mediated transfer of the human transforming growth factor beta1 encoding gene. Spine 1999;24:2419–25.
[3] Mochida J, Nishimura K, Nomura T, Toh E, Chiba M. The importance of preserving disc structure in surgical approaches to lumbar disc herniation. Spine 1996;21:1556–64.
[4] Buckwalter JA. Aging and degeneration of the human intervertebral disc. Spine 1995;20:1307–14.
[5] Horner HA, Urban JPG. 2000 Volvo Award in basic science: effect of nutrient supply on the viability of cells from the nucleus pulposus of the intervertebral disc. Spine 2001;26:2543–9.
[6] Antoniou J, Steffen T, Nelson F, Winterbottom N, Hollander AP, Poole RA, Aebi M, Alini M. The human lumbar intervertebral disc: evidence for changes in the biosynthesis and denaturation of the extracellular matrix with growth, maturation, ageing, and degeneration. J Clin Invest 1996;98(4):996–1003.
[7] Johnson WE, Roberts S. Human intervertebral disc cell morphology and cytoskeletal composition: a preliminary study of regional variations in health and disease. J Anat 2003;203(6):605–12.
[8] Maldonado BA, Oegema TR. Initial characterization of the metabolism of intervertebral disc cells encapsulated in microspheres. J Orthop Res 1992;10:677–90.
[9] Chiba K, Andersson GB, Masuda K. A new culture system to study the metabolism of the intervertebral disc in vitro. Spine 1998;23:1821–7.
[10] Gruber HE, Hanley Jr. EN. Human disc cells in monolayer vs 3D culture: cell shape, division and matrix formation. BMC Musculoskeletal Disord 2000;1(1):1.
[11] Gruber HE, Leslie K, Ingram J, Norton JH, Hanley EN. Cell-based tissue engineering for the intervertebral disc: in vitro studies of human disc cell gene expression and matrix production within selected cell carriers. Spine J 2004;4:44–55.
[12] Okuma M, Mochida J, Nishimura K, Sakabe K, Seiki K. Reinsertion of stimulated nucleus pulposus cells retards intervertebral disc degeneration: an in vitro and in vivo experimental study. J Orthop Res 2000;18:988–97.
[13] Nomura T, Mochida J, Okuma M, Nishimura K, Sakabe K. Nucleus pulposus allograft retards intervertebral disc degeneration. Clin Orthop 2001;389:94–101.
[14] Gruber HE, Johnson TL, Leslie K, Ingram JA, Martin D, Hoelscher G, Banks D, Phieffer L, Coldham G, Hanley Jr. EN. Autologous intervertebral disc cell implantation: a model using Psammomys obesus, the sand rat. Spine 2002;27:1626–33.
[15] Ganey T, Libera J, Moos V, Alasevic O, Fritsch KG, Meisel HJ, Hutton WC. Disc chondrocyte transplantation in a canine model: a treatment for degenerated or damaged intervertebral disc. Spine 2003;28:2609–20.
[16] Sakai D, Mochida J, Yamamoto Y, Nomura T, Okuma M, Nishimura K, nakai T, Ando K, Hotta T. Transplantation of mesenchymal stem cells embedded in Atelocollagen® gel to the intervertebral disc: a potential therapeutic model for disc degeneration. Biomaterials 2003;24:3531–41.
[17] Alini M, Li W, Markovic P, Aebi M, Spiro RC, Roughley PJ. The potential and limitations of a cell-seeded collagen/hyaluronan scaffold to engineer an intervertebral disc-like matrix. Spine 2003; 28:446–54.
[18] Mizuno H, Roy AK, Vacanti CA, Kojima K, Ueda M, Bonassar LJ. Tissue-engineered composites of anulus fibrosus and nucleus pulposus for intervertebral disc replacement. Spine 2004;29: 1290–7.
[19] Seguin CA, Grynpas MD, Pilliar RM, Waldman SD, Kandel RA. Tissue engineered nucleus pulposus tissue formed on a porous calcium polyphosphate substrate. Spine 2004;29:1299–306.
[20] Charriere G, Bejot M, Schnitzler L, Ville G, Hartmann DJ. Reactions to a bovine collagen implant. Clinical and immunologic study in 705 patients. J Am Acad Dermatol 1989;21:1203–8.
[21] Sakai D, Mochida J, Yamamoto Y, Toh E, Iwashina T, Miyazaki T, Inokuchi S, Ando K, Hotta T. Immortalization of human nucleus pulposus cells by a recombinant SV40 adenovirus vector: establishment of a novel cell line for the study of human nucleus pulposus cells. Spine 2004;29:1515–23.
[22] Uchio Y, Ochi M, Matsusaki M, Kurioka H, Katsube K. Human chondrocyte proliferation and matrix synthesis cultured in Atelocollagen gel. J Biomed Mater Res 2000;50:138–43.
[23] Ochi M, Uchio Y, Kawasaki K, Wakitani S, Iwasa J. Transplantation of cartilage-like tissue made by tissue engineering in the treatment of cartilage defects of the knee. J Bone Joint Surg B 2002;84:571–8.
[24] Kim YJ, Sah RL, Doong JY, Grodzinsky AJ. Fluorometric assay of DNA in cartilage explants using Hoechst 33258. Anal Biochem 1988;174:168–76.
[25] Collier S, Ghosh P. Comparison of the effects of nonstroidal antiinflamatory drugs (NSAIDs) on proteoglycan synthesis by articular cartilage explant and chondrocyte monolayer cultures. Biochem Phamacol 1991;41:1375–84.
[26] Farndale RW, Buttle DJ, Barrett AJ. Improved quantitation and discrimination of sulphated glycosaminoglycans by use of dimethylmethylene blue. Biochim Biophys Acta 1986;883:173–7.
[27] Urban JPG. Point of view. Spine 2004;29:1306–7.
[28] Roughley PJ. Point of view. Spine 2001;26:1752.
[29] Lee CK. Accelerated degeneration of the segment adjacent to a lumbar fusion. Spine 1988;13:375–7.
[30] Bao Q- B, McCullen GM, Higham PA, Dumbleton JH, Yuan HA. The artificial disc: theory, design and materials. Biomaterials 1996;17:1157–67.
[31] Urban JPG, McMullin JF. Swelling pressure of the intervertebral disc: influence of proteoglycan and collagen contents. Biorheol 1985;22:145–57.

Available online at www.sciencedirect.com
SCIENCE DIRECT®
Biomaterials 27 (2006) 335–345
Biomaterials
www.elsevier.com/locate/biomaterials

Regenerative effects of transplanting mesenchymal stem cells embedded in atelocollagen to the degenerated intervertebral disc

Daisuke Sakai[a,b,*], Joji Mochida[a,b], Toru Iwashina[a,b], Akihiko Hiyama[a,b], Hiroko Omi[a,b], Masaaki Imai[a,b], Tomoko Nakai[a,b], Kiyoshi Ando[b], Tomomitsu Hotta[b]

[a]*Department of Orthopaedic Surgery, Surgical Science, Tokai University School of Medicine, Bohseidai, Isehara, Kanagawa 259-1193, Japan*
[b]*Research Center for Regenerative Medicine, Tokai University School of Medicine, Bohseidai, Isehara, Kanagawa 259-1193, Japan*

Received 28 June 2005; accepted 30 June 2005
Available online 19 August 2005

Abstract

Intervertebral disc (IVD) degeneration, a common cause of low back pain in humans, is a relentlessly progressive phenomenon with no currently available effective treatment. In an attempt to solve this dilemma, we transplanted autologous mesenchymal stem cells (MSCs) from bone marrow into a rabbit model of disc degeneration to determine if stem cells could repair degenerated IVDs. LacZ expressing MSCs were transplanted to rabbit L2–L3, L3–L4 and L4–L5 IVDs 2 weeks after induction of degeneration. Changes in disc height by plain radiograph, T2-weighted signal intensity in magnetic resonance imaging (MRI), histology, immunohistochemistry and matrix associated gene expressions were evaluated between normal controls (NC) without operations, sham operated with only disc degeneration being induced, and MSC-transplanted animals for a 24-week period.

Results showed that after 24 weeks post-MSC transplantation, degenerated discs of MSC-transplanted group animals regained a disc height value of about 91%, MRI signal intensity of about 81%, compared to NC group discs. On the other hand, sham-operated group discs demonstrated the disc height value of about 67% and MRI signal intensity of about 60%. Macroscopic and histological evaluations confirmed relatively preserved nucleus with circular annulus structure in MSC-transplanted discs compared to indistinct structure seen in sham. Restoration of proteoglycan accumulation in MSC-transplanted discs was suggested from immunohistochemistry and gene expression analysis. These data indicate that transplantation of MSCs effectively led to regeneration of IVDs in a rabbit model of disc degeneration as suggested in our previous pilot study. MSCs may serve as a valuable resource in cell transplantation therapy for degenerative disc disease.
© 2005 Elsevier Ltd. All rights reserved.

Keywords: Intervertebral disc; Nucleus pulposus; Cell therapy; Tissue engineering; Regenerative medicine; Mesenchymal stem cells; Stem cell; Atelocollagen

1. Introduction

Low back pain is a chronic medical problem often associated with work disability and high health care costs [1,2]. Degeneration of the intervertebral disc (IVD), a major cause of low back pain, is an irreversible phenomenon with no currently available treatment [3]. Its etiology is unknown, but it can be described clinically as a loss of proper stability and mobility. Histopathologically, the IVD shows a decrease in water content associated with reduced proteoglycan content of the nucleus pulposus (NP), resulting in destruction of the annular structure and flattening of the disc [4,5]. Disc degeneration occurs naturally with age and circumstances secondary to various spinal disorders [6]. Moreover, there are many surgical procedures, such as

*Corresponding author. Department of Orthopaedic Surgery, Surgical Science, Tokai University School of Medicine, Bohseidai, Isehara, Kanagawa 259-1193, Japan. Tel.: +81 463 96 1121; fax: +81 463 96 4404.
E-mail address: daisakai@is.icc.u-tokai.ac.jp (D. Sakai).

0142-9612/$ - see front matter © 2005 Elsevier Ltd. All rights reserved.
doi:10.1016/j.biomaterials.2005.06.038

nucleotomy or a long vertebral fusion, in which degeneration in the operated site or even in the adjacent discs is accelerated, caused by reduction of the nucleus, increased axial loading, insufficient mobility and by other factors. Because almost no regeneration of the NP or the annulus fibrosus (AF) is possible [7], development of global methodologies to treat degenerated discs is needed.

Recent advances in molecular biology have provided new knowledge on the nature of the IVD and disc cells. Experimental studies on disc cell function have enabled scientists and clinicians to develop new approaches for the treatment of disc degeneration and regeneration [8]. Currently, strategies to regenerate the disc focus on restoring the ability to regulate matrix production and to restore the disc tissue. These include strategies involving cytokine and growth factor induction, gene therapy, tissue engineering and cell transplantation therapy [8–16].

Autologous NP cell transplantation has become one of the major techniques in attempts to prevent IVD degeneration in animal models [12–16]. However, in clinical situations, it has been considered difficult for broad application. One reason was that the procedure required more cells than can be harvested from a single disc. To overcome this problem, we have focused on the multi-lineage differentiation potential of mesenchymal stem cells (MSCs) as an alternative cell source for cell transplantation therapy of disc degeneration. There is an increasingly enthusiastic interest in stem cells as potential therapeutic reagents for various degenerative diseases and damaged organs [17]. MSCs are stem cells found in small numbers in the periosteum, cord blood or bone marrow [18]. They possess a unique ability to differentiate into various mesenchymal cell types [19,20]. Experimental MSC transplantation therapies are effective in a variety of diseases including the articular cartilage [20–26], and the induction of articular chondrocytes from MSCs in vitro is well established [27–29]. Because most of the cells that comprise the NP and AF in human adults express a chondrocyte-like phenotype, it is strongly suspected that disc cells are also likely to be induced from MSCs [30–33]. A pilot study on the feasibility of this procedure reported successful cell delivery using an atelocollagen gel as a cell-support scaffold [34]. MSCs were adequately delivered to the NP without major leakage using this approach. The study was followed for up to 8 weeks, and implantation was evaluated by histology and immunohistochemistry. Here, we followed the study up to 24 weeks after transplantation and assessed the regenerative effects of the procedure using plain radiography, magnetic resonance imaging (MRI), macroscopic findings, histology, immunohistochemistry and reverse transcription polymerase chain reaction (RT-PCR).

2. Materials and methods

Animal experiments were carried out according to a protocol approved by the Animal Experimentation Committee at our institution. Forty New Zealand white rabbits (mean weight 1.5 kg) were divided into three groups: 10 normal controls (NCs) without operations; 10 sham operated with only disc degeneration being induced; and 20 MSC transplantation animals, which were evaluated at 2, 4, 8, 16 and 24 weeks after transplantation (four at each time point).

2.1. Induction of degeneration in sham and MSC transplantation groups

Degeneration of the disc was induced under inhalation anesthesia using 2.5% isoflurane (Abbott Laboratories, North Chicago, IL, USA) in sham and MSC transplantation group rabbits 2 weeks before cell transplantation. NP tissue (5–8 mg wet weight) was aspirated from the IVDs at regions L2–L3, L3–L4 and L4–L5 using an antero-lateral approach with a 21-gauge needle on a 10 ml syringe, as described previously [34].

2.1.1. MSC isolation and culture

MSCs were isolated from rabbit bone marrow by the gradient isolation of mononuclear cells and cell attachment to tissue culture plastic as described previously [34]. Under inhalation anesthesia, marrow blood was collected by aspiration from the iliac crest of the MSC transplantation group rabbits via an 18-gauge needle, collecting 10 ml of marrow blood into 1000 U of heparin. The marrow blood was filtered through a cell strainer for excluding any fatty tissues and blood clots, and then carefully poured over 20 ml of Nycoprep™ 1.077 Animal (Axis-Shield PoC AS, Oslo, Norway) and centrifuged at 600*g* for 30 min. Mononucleated cells were recovered from the middle layer, washed three times with phosphate-buffered saline (PBS) and cultured until they reach approximately 80% confluence over about 12–15 days in 25 cm^2 flasks in low-glucose Dulbecco's modified Eagle's medium (DMEM, Gibco, Green Island, NY, USA) containing 10% fetal bovine serum (Gibco) and antibiotics (penicillin G, 100 U/ml; streptomycin, 0.1 mg/ml; amphotericin B, 0.25 μg/ml) at 37 °C under 5% CO_2.

2.1.2. In vitro differentiation assays of the MSCs

The MSCs were checked for multi-linage differentiation by adipogenic, chondrogenic and osteogenic differentiation assays as described previously [22]. Briefly, adipogenesis was induced by induction medium including high-glucose DMEM, 100 nM dexamethasone, 200 μM indomethacin (Wako Pure Chemical Industries, Ltd., Osaka, Japan), 10 μg/ml insulin (Sigma Chemical Co., St Louis, MO, USA) and 500 μM 3-isobutyl-1-methylxanthine (Wako). Induction was confirmed by Oil red O staining. For chondrogenesis, MSCs were pelleted by centrifugation (800*g*, 5 min) and cultured in induction medium including high-glucose DMEM, 1% ITS+ (Beckton Dickinson, Franklin Lakes, NJ, USA), 100 nM dexamethasone, 50 μM ascorbic acid 2-phosphate, 35 μg/ml proline (Sigma) and 5 ng/ml TGF-β1 (Sigma). The pellet was cultured for 21 days, then made into frozen sections, and evaluated by immunostaining for type II collagen and keratan sulfate. Osteogenesis was induced by culturing MSCs monolayered in medium

containing 100 nM dexamethasone (Sigma), 10 mM β-glycerol phosphate (Sigma), and 50 μM ascorbic acid 2-phosphate (Wako). Alkaline phosphatase staining and calcium deposition shown by Von Kossa staining were evaluated histochemically.

2.2. Preparation and transplantation of MSCs

The cultured MSCs used for transplantation were infected with Ad-*LacZ*, a recombinant adenovirus vector expressing the *Escherichia coli LacZ* gene as described previously [34,35]. The MSCs were infected overnight with 1×10^4 PFU ml^{-1} of Ad-*LacZ* at a multiplicity of infection of 20: a concentration that infects more than 90% of the cells without effecting cell viability. Samples of infected cells were stained with 0.1% 5-bromo-4-chloro-3-indolyl-B-D-galactopyranoside (X-gal; Sigma) following a PBS wash proving that nearly 100% of the cells were infected. An atelocollagen gel (KOKENCELLGEN; Koken Co., Ltd., Tokyo, Japan) solution composed of 0.3% type II collagen was used as a carrier because it is the main collagen composing the IVD. The atelocollagen gel is known to have advantages over other cell-supporting scaffolds for its low immunoreactivity and ease of handling, as it is in liquid form when cooled and hardens when warmed to body temperature. The gene-labeled MSCs were embedded in this solution, adjusted with DMEM, HEPES (Sigma) and $NaHCO_3$ (Sigma), to a final cell density of 1×10^6 cell/ml, and used for transplantation immediately. Transplantation was performed into degeneration-induced discs of the MSC transplantation group rabbits under inhalation anesthesia. Using an insulin micro-injector with a 27-gauge needle, 40 μl of mildly cooled MSC/atelocollagen implant in a runny form was injected carefully.

2.3. Radiographic and MRI analysis

Lateral plain radiographs were taken under anesthesia inhalation in all groups before harvest, using a DHF-155H high potential generator (Hitachi Medical Corporation, Tokyo, Japan). Vertebral body heights and disc heights were measured using NIH image software (NIH, freeware at: http://rsb.info.nih.gov/nih-image/). The disc height index (DHI) described by Lu et al. [36] was calculated for comparisons between groups. Changes in the DHI were expressed as %DHI and normalized to the measured preoperative IVD height (%DHI = postoperative DHI/preoperative DHI × 100). MRI images were also taken using a Vectra Fast 1.5-T imager (Yokogawa GE Medical Systems, Japan). The rabbits were positioned supine on a quadrature surface coil and sagittal images through the lumbar spine were obtained (spin echo; repetition time 3200 s; echo time 130 s; number of excitations 20; field of view 14 cm; slice thickness 3 mm; no phase wrap). The signal intensity of each disc on T2-weighted image was scanned as TIFF image and quantified with a CS Analyzer version 2.01 software (Atto Biotechnologies Inc., Tokyo, Japan) using garlic oil supplement capsules (Garlic Oil; Nature Made, Mission Hills, CA) as standard control markers.

2.4. Macroscopic findings

At 2, 4, 8, 16 and 24 weeks after transplantation, four rabbits from the MSC transplantation group and two rabbits each from the NC and sham-operated groups were euthanized with an excess dose of pentobarbital (Euthanasia B solution: Henry Schein Inc., Washington Port, NY) and their spines harvested. L2/3 discs were isolated with both upper and lower vertebral bodies completely attached. They were fixed in 10% formalin neutral buffer solution (Wako), decalcified in Plant-Rychlo solution (Decalcifying Solution A; Wako) and dehydrated in a graded series of ethanol (70%, 90%, 99%, Wako). L2/3 discs with vertebral body units were cut longitudinally at the center of the disc for macroscopic evaluation. L3/4 discs were harvested mainly to make frozen sections for X-gal staining and L4/5 discs were used for extracting total RNAs for RT-PCR.

2.5. Histology

After macroscopic evaluation, L2/3 discs and some of L3/4 discs were processed individually for paraffin wax embedding. The paraffin blocks were sectioned longitudinally using a micro-tome into 4 μm sections. These were stained with hematoxylin and eosin, and Safranin-O for evaluation. A histological grading system for disc degeneration, devised by Nishimura and Mochida [12] focusing on the morphological changes in the annular structure, was used for evaluation of degenerative changes (Fig. 4b). Two histologists who are familiar with human and animal IVD specimens performed evaluation of these sections, with their intra-observer error being minimum.

Oil red O and Von Kossa staining for identification of lipid and calcium deposition was also performed and evaluated to assess any possible adipogenesis or osteogenesis in the MSC-transplanted discs.

2.6. Immunohistochemistry

To evaluate whether discs of MSC transplantation group had regained proteoglycan synthesis, immunohistochemical staining for keratan sulfate was carried out on all sections. Methanol–H_2O_2 treatment was applied for the elimination of autogenous peroxidase reaction and 10% normal goat serum was used for blocking of non-specific immunoreaction. Sections were labeled overnight at 4 °C with anti-rabbit keratan sulfate monoclonal antibody (Chemicon, Temecula, CA, USA), prepared at a dilution of 1:200 in PBS. This antibody recognizes short peptides substituted with keratan sulfate side chains of proteoglycan in human articular cartilage that cross-react with rabbit keratan sulfate. The samples were washed three times with PBS and reacted with mouse anti-horseradish peroxidase (HRP: Dako A/S, Profuktionsvej, Denmark) at a dilution of 1:100 in PBS for 30 min at 4 °C. Finally, the sections were counter stained with hematoxylin. Cartilage of the femoral head served as a positive control and skeletal muscle as a negative control.

2.7. RT-PCR of matrix-specific genes of the disc

Total RNAs were isolated from L4/5 discs immediately after harvest. Briefly, discs were minced in pieces using a sterile scalpel then snap-frozen and pulverized in liquid nitrogen. The tissue powder was homogenized with Isogen reagent (Nippon-gene, Tokyo, Japan) according to the manufacturer's

instructions and further purified using RNeasy spin columns (Qiagen, Valencia, CA, USA). Absorbances at 260 and 280 nm were measured for RNA quantification and quality control. RNA samples were then reverse transcribed to cDNA using Oligo dT primers and Multiscribe Reverse Transcriptase (Applied Biosystems, Foster City, CA, USA) followed by specific amplification of matrix-specific genes. Primers were designed with Primer3 software (MIT, free download at: http://www-genome.wi.mit.edu/cgi-bin/primer/primer3_www.cgi) using sequence data from the National Center for Biotechnology Information GenBank database. Primers for type II collagen, aggrecan and versican, the main components of the disc extracellular matrix, and glyceraldehyde-3-phosphate dehydrogenase (GAPDH) that served as an internal control, were obtained from Invitrogen (Carlsbad, CA). The upstream and downstream primer sequences for each primers were as follows: GAPDH: 5′-TCA CCA TCT TCC AGG AGC GA-3′, 5′-CAC AAT GCC GAA GTG GTC GT-3′; type II collagen-α 1 chain: 5′-AAC ACT GCC AAC GTC CAG AT-3′, 5′-CTG CAG CAC GGT ATA GGT GA-3′; aggrecan: 5′-GAG GAG ATG GAG GGT GAG GTC TTT-3′, 5′-CTT CGC CTG TGT AGC AGC TG-3′; versican: 5′-TTA TGT GGA TCA TCT GGA CGG-3′, 5′-GCA TCC AAG AGC CAC CCA-3′.

PCR amplification was carried out using a two-step protocol of 10 min pre-PCR heat step at 95 °C for activation of Ampli*Taq* Gold DNA polymerase (Applied Biosystems), followed by 40 cycles of denaturing at 95 °C for 15 s and annealing at 60 °C for 1 min. The PCR products were separated electrophoretically using non-denaturing 1.2% TBE poly-acrylamide gels and stained with ethidium bromide. The gels were scanned under UV light with a Densitograph system (Atto) and the band intensities were quantified densitometrically and normalized to GAPDH using CS Analyzer version 2.01 (Atto).

2.8. Evaluation for cell survival of MSCs by X-gal staining

One L3/4 disc from MSC transplantation group at each time point was frozen immediately after harvest and cryosectioned at 5 μm. Sections were fixed with 4% paraformaldehyde in PBS, rinsed in PBS and incubated overnight with X-gal substrate (Sigma) at 37 °C.

2.9. Statistical analysis

A comparison of group means between NC group, sham group and MSC-transplanted group was determined using the repeated measure ANOVA and Fisher's LSD post hoc test. Statistical significance was determined based on $P<0.05$. Error bars were set to represent standard deviation (SD).

3. Results

Differentiation assay results demonstrated sufficient differentiation of autologous MSCs in three different lineages. Vector incorporation in the MSCs used for transplantation was more than 90% (data not shown).

Radiographic analysis demonstrated significant disc space narrowing 4 weeks after the induction of IVD degeneration in sham and MSC transplantation groups. The mean DHI in sham-treated rabbits continued to decrease until 6 weeks after the induction of IVD degeneration and then plateaued. With a mean DHI for NC group at beginning of the study expressed as 100%, the mean DHI of the sham group was 64±2% at 6 weeks after induction and 67±4% at 26 weeks. In contrast, the MSC transplantation group demonstrated a significant increase in the DHI 10 weeks after

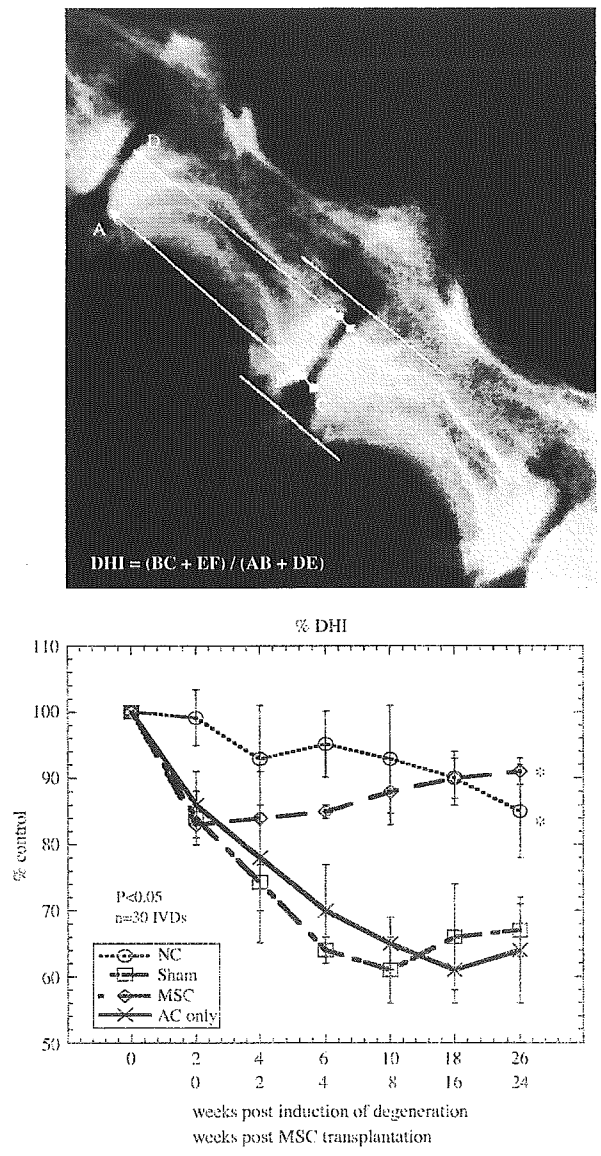

Fig. 1. A representative lateral radiograph image of MSC-transplanted animal disc and measurement protocol of disc height index (DHI). Restoration of DHI began 4 weeks after MSC transplantation while sham animal discs showed constant decrease. Data for animals with atelocollagen (AC) injected, but without cells, are also shown for comparison.

induction (8 weeks after MSC transplantation). Two weeks after induction it was 83±3%, 85±1% at 6 weeks, 88±5% at 10 weeks, 90±4% at 18 weeks and 91±2% at 26 weeks ($P<0.05$) (Fig. 1).

MRI T2-weighted signal intensities in the sham-treated and MSC transplantation groups decreased significantly shortly after the induction of IVD degeneration, with only the MSC transplantation group restored after MSC transplantation. For the sham-operated groups figures were 72±6% 2 weeks after induction, 64±8% 6 weeks after induction, 62±8% at 10 weeks, 56±5% at 18 weeks and 60±4% at 26 weeks. For the MSC transplantation group the figures were 70±6% at 2 weeks, 80±8% at 6 weeks after induction (4 weeks after transplantation), 82±4% at 10 weeks, 84±6% at 18 weeks and 81±2% at 26 weeks ($P<0.05$) (Fig. 2).

From macroscopic evaluations, discs from NC group showed an intact NP without narrowing of the disc space, whereas discs from sham-operated rabbits showed NP with connective tissue invasion accompanied by apparent disc space narrowing. The MSC-transplanted group discs demonstrated reappearance of the NP with restoration of disc space narrowing (Fig. 3).

Histological analysis also proved significant regenerative effects of the procedure. NC group discs show oval-shaped nucleus with no collapse of the inner annular structure. Sham-operated discs show collapse

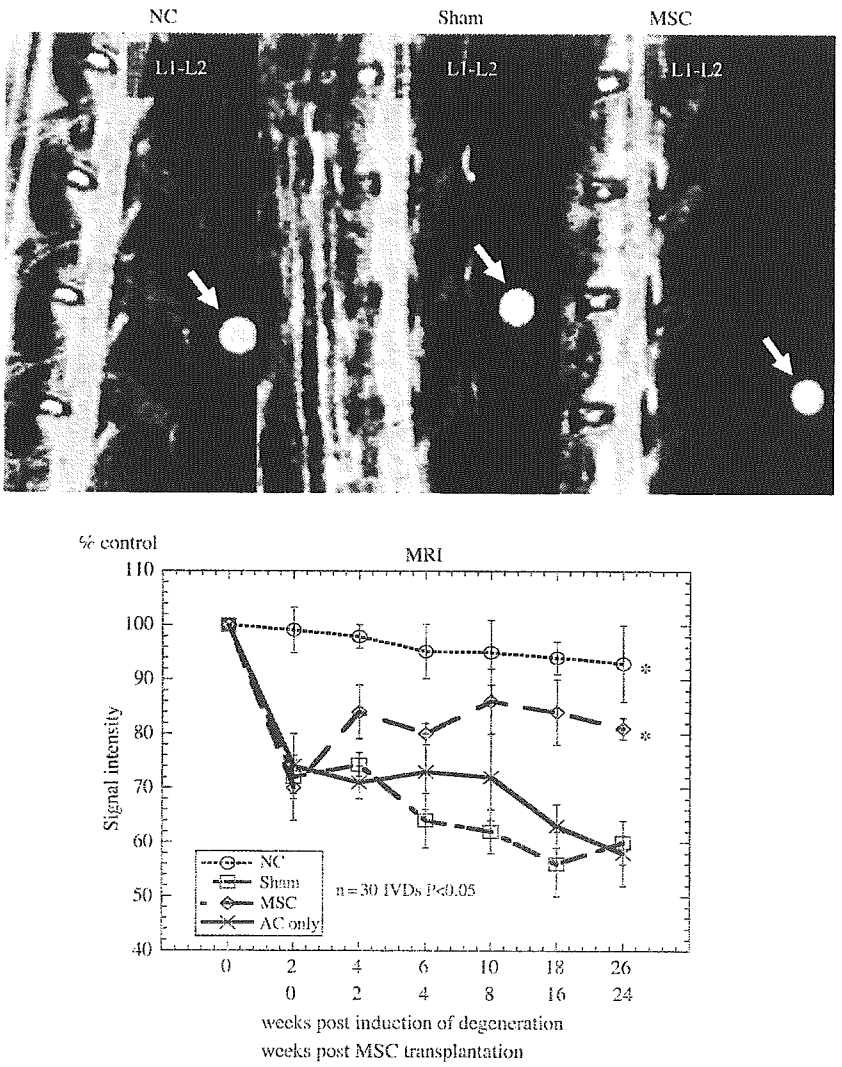

Fig. 2. MRI image of normal control, sham and MSC-transplanted animals taken 26 weeks post-induction of degeneration (24 weeks after MSC transplantation in MSC-transplanted animals). Images of sham and MSC-transplanted animals are among the best model obtained by means of degeneration and restoration. Significant recovery of T2-weighted signal intensity is seen in L2–L3, L3–L4 and L4–L5 discs of MSC-transplanted discs compared to very low signal intensity in sham. The arrows indicate the garlic oil supplement capsules used for standardizing control. Data for animals with atelocollagen (AC) injected, but without cells, are also shown for comparison.

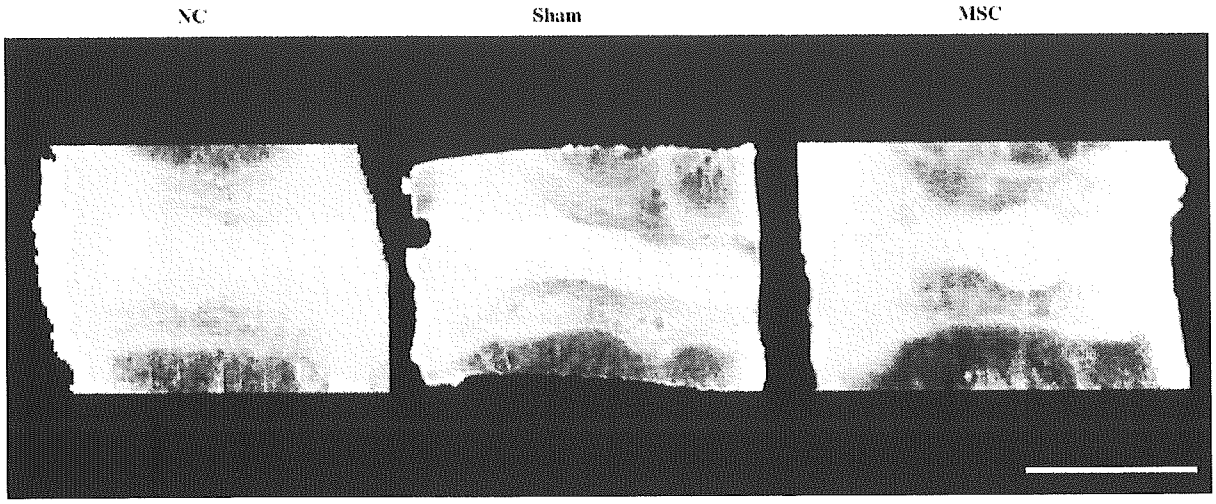

Fig. 3. Macroscopic view of normal control, sham-operated and MSC-transplanted discs harvested at period equivalent to 24 weeks after MSC transplantation in the MSC transplantation group. Note that depletion of nucleus and disc height narrowing is evident in sham group disc, but not so apparent in MSC-transplanted group disc. Bar = 5 mm.

of the inner annulus morphology from 4 weeks (6 weeks after induction of degeneration). Fibrosis in the nucleus due to cell invasion from the surrounding region is completed at 24 weeks. MSC group discs showed relatively preserved inner annulus structure with minimal fibrosis in the nucleus region (Fig. 4a). Disc degeneration grading results showed that MSC transplantation group discs were graded as 1–2 at the most, compared with 4–5 in the sham-operated group. NC group discs maintained grade 0 throughout the study (Fig. 4b and c). Close observation of the sections demonstrated that cells composing the NP in the discs of the MSC transplantation group expressed two distinct cell types: spindle-shaped cells with mildly dense matrix and large oval-shaped cells with occasional vacuoles. Vertebrae from the sham-operated rabbits showed replacement of the disc with fibrosis and dense extra cellular matrix.

No apparent depositions of lipid or calcium were noted in the nucleus of MSC-transplanted discs showing absence of adipogenesis and osteogenesis. Safranin-O staining and immunohistochemistry results revealed staining patterns similar to normal discs in the MSC transplantation group discs, whereas the sham-operated group discs stained poorly (Fig. 5a and b). This was further confirmed at the mRNA level. RT-PCR analysis of the discs harvested 24 weeks after transplantation showed significant upregulation of both aggrecan and versican gene expression. Type II collagen genes were also restored ($P<0.05$, Fig. 6).

X-gal staining of MSC-transplanted discs 2 weeks after transplantation demonstrated that $27\pm8\%$ of the cells seen in NP were positively stained. The mean percentage of X-gal positive cells increased significantly up to $72\pm12\%$ by 8 weeks after transplantation, thus proving survival and proliferation ($P<0.05$, Fig. 7). X-gal positive cells gradually decreased in sections harvested 8 weeks after transplantation, because adenovirus-mediated *LacZ* gene transfer is transient.

4. Discussion

The multi-lineage differentiation potential and highly viable nature of stem cells has provided many potential techniques to treat various diseases [37]. Clinically, MSC transplantation has become one of the treatment options for full-thickness articular cartilage defects, osteogenesis imperfecta and myocardial infarction, while applications to other diseases are being developed [23–27]. The advantages of MSC transplantation over other cell transplantation therapies is because MSCs are easy to harvest, isolate and grow, with minimum involvement of in vitro techniques [19]. Moreover, MSCs are considered suitable not only for autologous but also allogeneic transplantations, as they lack the expression of HLA class II antigens [20]. Consequently, MSCs serve as a practical cell source widely applicable in clinical settings. Despite such an interest and the growing number of research data, studies directed toward regeneration of the IVD have only just begun.

An atelocollagen gel solution was used here for the cell delivery scaffold because it allows embedded cells to grow in a three-dimensional environment, which is very suitable for disc cells and chondrocytes in vitro [8,31]. Our pilot study on the feasibility of using this scaffold resulted in successful cell delivery [34]. Atelocollagens are clinically safe collagen solutions with reduced